

SARS coronavirus protein nsp1 disrupts localization of Nup93 from the nuclear pore complex

Garret N. Gomez, Fareeha Abrar, Maya P. Dodhia, Fabiola G. Gonzalez and Anita Nag*
Furman University, 3300 Poinsett Highway, Greenville, SC 29613

Running Title: *nsp1 alters nuclear pore complex*

Key Words: SARS-CoV, nsp1, Nup93, nuclear pore complex, NLS, immunofluorescence

*To whom correspondence should be addressed: Anita Nag, Departments of Biology and Chemistry, Furman University, 3300 Poinsett Highway, Greenville, SC 29613; anita.nag@furman.edu; Tel: 864-294-2354

ABSTRACT: Severe acute respiratory syndrome coronavirus nonstructural protein 1 (nsp1) is a key factor in virus-induced down-regulation of host gene expression. In infected cells, nsp1 engages in a multi-pronged mechanism to inhibit host gene expression by binding to the 40S ribosome to block the assembly of translationally competent ribosome, and then inducing endonucleolytic cleavage and the degradation of host mRNAs. Here, we report a previously undetected mechanism by which nsp1 exploits the nuclear pore complex and disrupts nuclear-cytoplasmic transport of biomolecules. We identified members of the nuclear pore complex from nsp1-associated protein assembly and found that expression of nsp1 in HEK cells disrupts Nup93 localization around the nuclear envelope without triggering proteolytic degradation, while the nuclear lamina remains unperturbed. Consistent with its role in host shutoff, nsp1 alters the nuclear-cytoplasmic distribution of a RNA binding protein, nucleolin. Our results suggest that nsp1, alone, can regulate multiple steps of gene expression including nuclear-cytoplasmic transport.

INTRODUCTION

The nuclear pore complex (NPC) modulates nuclear cytoplasmic translocation of biomolecules in a selective manner by perforating the nuclear envelope that creates a barrier between the nucleus and the cytoplasm, essentially separating transcription from translation in eukaryotic cells (Ibarra *et al.* 2016; Knockenhauer and Schwartz 2016). The NPC, a dynamic, intricate multi-protein machine (about 125 MDa) functions by allowing selective passage of protein and RNA-protein complexes. Serving as the only gate-keeper between the nucleus and the cytoplasm for biomolecules larger than 30 kDa, the NPC maintains cellular order and is often disrupted by viruses to control nuclear-cytoplasmic transport. The NPC is made of about 30 different proteins that arrange in repetitive structures, yielding a complex assembly of eight fold symmetry, and it consists of a central ring that forms a cylindrical passage, basket-like nuclear extension and cytoplasmic filaments. Several members of DNA viruses alter the NPC by directly interacting with one or more NPC-associated proteins so that the virus can synthesize, process, and transport its own mRNA (Ao *et al.* 2012; Di Nunzio *et al.* 2012; Copeland, Newcomb and Brown 2009). RNA viruses that are primarily confined in the cytoplasm are less likely to disrupt the NPC (Mühlbauer *et al.*, 2015; Le Sage and Mouland, 2013). Cytoplasmic viruses tend to translocate host nuclear proteins to the cytoplasm to promote successful viral replication and translation. The severe acute respiratory syndrome coronavirus (SARS-CoV), a positive strand RNA virus, is reported to disrupt host gene expression by blocking ribosome assembly and promoting host mRNA degradation in the cytoplasm. Here, we report that SARS-CoV induces nucleoplasmic accumulation of nucleoporin Nup93, and alters the composition of the NPC.

SARS-CoV is an enveloped, positive-stranded RNA virus containing a single-stranded RNA genome of about 29.7 kb long, and is a member of a large viral genome order known as the Nidovirus (Sevajol *et al.* 2014). While most coronaviruses cause mild respiratory syndrome, an outbreak of SARS-

CoV in 2003 created a major epidemic by resulting in a 10% fatality rate followed by an outbreak of Middle East Respiratory Syndrome Coronavirus (MERS-CoV, 36% fatality) in 2014 (Lokugamage *et al.* 2015; Sevajol *et al.* 2014). SARS-CoV genome encodes a total of 16 nonstructural proteins, few with experimentally proven functions in the host cell. Among them, nonstructural protein 1 (nsp1) is a 19-kDa protein that possesses a unique mechanism to down regulate host gene expression during viral infection. Using a two-pronged strategy to dampen host gene expression, nsp1 binds to the 40S ribosome at the 5'-untranslated region (UTR) of host mRNA and stalls further ribosome assembly, ultimately inhibiting host protein synthesis. Furthermore, nsp1 seizes an unknown cellular endonuclease to cleave mRNA at the 5'-UTR, facilitating rapid decay of the cleaved mRNA by exonucleases (Huang *et al.* 2011; Kamitani *et al.* 2006; Kamitani *et al.* 2009; Lokugamage *et al.* 2012; Narayanan *et al.* 2008).

Here, we report a previously undetected role of nsp1 in deregulating the host cell's function by disrupting the composition of the nuclear pore complex and by altering the localization of a RNA binding protein. We present results that demonstrate nsp1 associates with Nup93 and displaces it from the NPC. Nup93 delocalization is dependent on the presence of nsp1 in the cell. We also show that the localization of RNA binding protein, nucleolin, has been altered to the cytoplasm. These results offer a new mode of function by nsp1 in suppressing host cell's function.

RESULTS

Nuclear pore complex proteins are identified in nsp1 complex

Nsp1 induces translational shutoff and endonucleolytic cleavage at the 5'-UTR of mRNAs to suppress host gene expression. 218 amino acids long, nsp1 binds to the 40S ribosome and also seizes a cellular endonuclease to cleave host mRNA in a two-pronged mechanism that down-regulates protein synthesis from host mRNA. Multiple mutations on the surface residues of nsp1 differentially inhibit gene expression (Jauregui *et al.* 2013). Additional experiments characterized two mutants carrying specific point mutations at positively-charged amino acid residues: i) an active mutant R124A/K125A, which binds to the 40S ribosome and inhibits host protein synthesis, but fails to cleave mRNA (Tanaka *et al.* 2012), and ii) an inactive mutant K164A/H165A, which neither binds to the 40S ribosome nor cleaves the mRNA (Huang *et al.* 2011; Kamitani *et al.* 2009). We performed a quantitative proteomic assay to compare host proteins that exclusively bind to nsp1 and R124A/K125A, but fails to bind to K164A/H165A to identify key cellular proteins that help nsp1 inhibit protein translation. Nsp1 and each mutant (R124A/K125A and K164A/H165A) proteins were separately expressed and purified from *E. coli* using a glutathione S-transferase (GST) tag, and were then used to isolate host protein complexes from HEK whole cell extract. As expected, both nsp1 and R124A/K125A bind greater number of cellular proteins relative to the K164A/H165A mutant (Fig. S1, lanes 6 and 7 to lane 8). Peptides that are present in K164A/H165A were excluded to eliminate nonspecific binding of cellular proteins to GST as well as to identify proteins that are functionally relevant to nsp1's ability to suppress host gene expression. Proteins that are only present in functionally active nsp1 or show a minimum of 3-fold enhancement compared to K164A/H165A were considered for further study (see below). K164A/H165A mutant serves as the most suitable control since this mutant is unable to carry out host shutoff.

Among nsp1-associated proteins identified by mass spectrometry, we detected two members of the nuclear pore complex, Nup93 and Nup210L. The unique peptide corresponding to Nup93 encompassed first 31 amino acid of the protein (see materials and methods). To independently confirm Nup93 binding to nsp1 in HEK cells, we expressed Myc-tagged nsp1 and K164A/H165A in HEK cells and optimized nsp1 expression. As expected, indirect immunofluorescence experiments showed that the majority of nsp1 was localized in the cytoplasm (Kamitani *et al.* 2006). However, we also found that a small fraction of nsp1 was localized in the nucleus (Fig. 1A). We were unable to establish a stable cell line expressing nsp1 due to its host shutoff properties and carried all experiments by transiently transfecting cells for nsp1 expression. Therefore, most of our experiments were conducted 24 hours post-transfection to record the maximum effect of nsp1 in the cell and were performed under the condition when majority of cells (over 99%) showed nsp1 expression (Fig. 1A and B). We found that nsp1

expression diminished significantly beyond 24 hours when the protein was expressed by transient transfection, likely due to nsp1-mediated suppression of protein expression from nsp1 mRNA (see below). Myc-nsp1 and myc-K164A/H165A expressing cells were used for immunoprecipitation. Anti-myc pull down of nsp1 showed co-immunoprecipitation of Nup93 relative to cell extracts from mock expressed cell (Fig. 1C), while K164A/H165A pull down showed significantly decreased level of Nup93 compared to nsp1 (Fig. 1D). To establish that myc-IP does not pull down non-specific ribosome associated proteins, and is similar to the protein composition identified in the mass spectrometry, we tested the binding of ribosomal protein 10 (rps10), which was not detected in the mass spectrometry. Myc-IP followed by the western blot verified the absence of rps10, confirming the validity of myc-pull down experiments.

Nup93 and Nup210 are part of a ring structure of the NPC and serve as linkers between other proteins present in the complex. Nup93 serves as the scaffold of the NPC and maintains correct structure of this complex (Grandi *et al.* 1997; Vollmer and Antonin 2014). To detect if nsp1 expression in HEK cells has any effect on the NPC, we examined the localization of Nup93 using indirect immunofluorescence in the presence and absence of nsp1. As expected, in the absence of nsp1, Nup93 localized on the nuclear envelope and displayed clear fluorescence staining around the nucleus (Fig. 2A, top panel). However, in the presence of nsp1, Nup93 localization significantly shifted from the nuclear envelope to the nucleoplasm, showing that nsp1 is able to alter subcellular localization of NPC components (Fig. 2A, middle panel). Expression of K164A/H165A did not meaningfully alter Nup93 staining on the nuclear envelope (Fig. 2A, bottom panel). Quantitative analysis of nucleoplasmic density of Nup93 from the Z-stack images show over 2 fold increase in the Nup93 density in the nucleoplasm for nsp1 expressing cells (Fig. 2B and C, see the table for average density). We did not notice any significant difference in Nup93 signal in the nucleoplasm in K164A/H165A expressing cells relative to no expression samples. Since Nup93 peptide was isolated in R124A/K125A mutant complex but not in the K164A/H165A complex, we expect the R124A/K125A to alter accumulation of Nup93 to the nucleoplasm similar to wild type nsp1. Additionally, we performed nuclear cytoplasmic fractionation of cells expressing nsp1 and K164A/H165A mutant and verified fractionation efficiency by the presence of hnRNPK in the nucleus and GAPDH in the cytoplasm (Supplementary Fig. S2). Nuclear cytoplasmic fractionation of cells identified Nup93 primarily in the nucleus even in the presence of nsp1 (Fig. 2D). We conclude, Nup93 displaces from the nuclear envelope to the nucleoplasm where a small population of nsp1 associates with Nup93 instead of the cytoplasm where the majority of nsp1 accumulates.

The composition of NPC is altered in the presence of nsp1

Next we investigated if the nuclear membrane architecture was still intact in the presence of nsp1 by examining the Lamin A/C protein. Lamin A/C are filament proteins that provide strength and structure to the nuclear envelope (Naetar, Ferraioli and Foisner, 2017). Using indirect immunofluorescence against Lamin A/C, we confirmed that the nuclear lamina stays intact in the presence of nsp1 (Fig. 3A). Next, we examined if other members of the nuclear pore complex are also displaced from the nuclear envelope by detecting localization of Nup88, which is localized in the cytoplasmic filament of the (Bernad *et al.* 2004; Bernad *et al.* 2006) NPC in the absence of nsp1 (Fig. 3B). Although there was a modest decrease in overall intensity of Nup88, we concluded that majority of Nup88 (Nup205, Supplementary Fig. S3) localization did not significantly alter in the presence of nsp1 (Fig. 3B). These results suggest that nsp1 alters the composition of the NPC but does not disrupt the entire complex. Although we do not know how the rest of the protein subunits of the NPC are held together, selective displacement of nucleoporins is not uncommon during viral infection and has been reported in the adenovirus, HIV, and poliovirus (Le Sage and Moulard 2013).

Altered localization of Nup93 is dependent on the presence of nsp1

Since Nup93 localization at the nuclear envelope was altered upon nsp1 expression, we examined if Nup93 is degraded in the presence of nsp1 by proteasome-mediated degradation. We monitored the

level of Nup93 after inhibiting production of newly synthesized Nup93 by treating HEK cells with cyclohexamide following nsp1 expression. Our results show that Nup93 is not degraded in the presence of nsp1 (Fig. 4A), suggesting that Nup93 is selectively displaced from the NPC to the nucleoplasm without any degradation.

Transient transfection of HEK cells with nsp1 expression plasmids allowed us to study the effect of nsp1 for the time period pertaining to significant expression of the protein. However, expressed nsp1 protein confers the same inhibitory effect on its own mRNA as to other host mRNAs in the cell. We found that 40 hours post-transfection, very little nsp1 was made while K164A/H165A expression continued (Figs. 1B and 4B). We used this observation to our advantage and examined localization of Nup93 at 0, 12, 24, and 48 hours post-transfection with nsp1 expression plasmids. As expected from our previous results, we found Nup93 localization gradually altered from the nuclear envelope to the nucleoplasm at 12 and 24 hours post-transfection. However, at 48 hours, when very little nsp1 protein was present, Nup93 reconvened at the nuclear envelope showing immunostaining around the nucleus (Fig. 4C). Quantitative analysis of Nup93 intensity in the nucleoplasm shows gradual increase up to 24 hours. The reduced nucleoplasmic density of Nup93 after 48 hours correlates with its presence on the nuclear envelope and absence of nsp1 (Fig. 4D). These results confirm that Nup93 does not undergo rapid degradation in the presence of nsp1, but rather displaced in the nucleoplasm when nsp1 levels are substantial.

Nuclear cytoplasmic distribution of proteins changes upon nsp1 expression

The results presented above are consistent with a model that suggests nsp1 manipulates the nuclear pore complex to disrupt nuclear-cytoplasmic shuttling of cellular proteins shown in other viruses (Waggoner and Sarnow 1998; McBride, Schlegel and Kirkegaard 1996; Borah *et al.* 2011). In order to investigate if RNA binding proteins have altered localization in the presence of nsp1, we carried out nuclear and cytoplasmic fractionation followed by protein extraction from each cellular fraction. We observed hnRNP, a poly(C)-binding protein is exclusively present in the nuclear fraction while GAPDH was primarily cytoplasmic, affirming our method of fractionation of nuclear and cytoplasmic proteins (Fig. Supplementary Fig. S2). We detected cellular localization of several RNA binding proteins including hnRNP and hnRNP E1/E2, but did not observe any difference in their localizations in the presence of nsp1. However, nucleolin selectively accumulated in the cytoplasm (Figs. 5A and B) resulting 40% decrease of nucleolin from the nucleus to the cytoplasm. Since nucleolin has a bipartite nuclear localization signal (NLS), we analyzed any global disruption of protein import by classical NLS-mediated pathway by using an EGFP containing reporter carrying tandem NLS signals. Due to the presence of tandem NLS repeats, this protein (larger than 30 kDa) depends on the classical NLS-mediated import pathway to enter the nucleus (Gustin and Sarnow 2001). We did not find any change in the localization of the EGFP protein to the nucleus in the presence of nsp1 (Supplementary Fig. S4) ruling out any global effect on protein localization by nsp1. Even though we cannot rule out altered localization of other cellular proteins, our results suggest that nsp1 exploits the NPC and alters the localization of nucleolin.

DISCUSSION

SARS coronavirus nsp1 has been studied extensively for its role in host shutoff via translational inhibition and mRNA cleavage. We identified an uncharacterized function of nsp1 in disrupting the nuclear pore complex by altering the localization of Nup93. Using immunofluorescence, we showed that localization of Nup93 changes while Nup88 and Lamin A/C remain largely unaffected. Moreover, the presence of nsp1 alters nuclear-cytoplasmic distribution of nucleolin, which has been reported to be a key factor in RNA stability. Our results demonstrate that expression of nsp1 aids disruption of the nuclear-cytoplasmic localization of nucleolin. Nucleolin is a sequence-specific RNA binding protein that has been implicated in maintaining RNA stability (Ghisolfi-Nieto *et al.* 1996). Given the role of nsp1 in destabilizing majority of mRNA in the cell while the viral mRNA remains stable, suggests a possibility

that nucleolin may modulate mRNA stability by differential binding to different RNA sequences in the presence of nsp1.

The NPC, a 125 MDa protein assembly composed of 30 different proteins, forms a formidable barrier for macromolecules while allowing free passage for water, ions, and nucleotides (Knockenbauer and Schwartz 2016). These multi-protein complexes perform a highly selective mechanism to allow specific cargo in and out of the nucleus by distinct mechanisms based on the nuclear import and export signals present in these complexes. The NPCs regulate transportation of nuclear localization signal (NLS)-containing proteins, M9 sequence-containing proteins, and several types of RNA mediated by chromosome region maintenance 1 (CRM1). Viral subversion of the NPC and virus-induced modification of nucleoporins have been reported in poliovirus, herpesvirus, and adenovirus (Le Sage and Mouland 2013). Poliovirus infection induces reduction of nucleoporins in the NPC (Gustin and Sarnow, 2001). A change in the NPC composition is observed during rhinovirus-induced degradation of Nup62, Nup98, and Nup153 (Gustin and Sarnow 2001; Gustin and Sarnow 2002; Park *et al.* 2008; Park, Skern and Gustin 2010). Similarly, cardiovirus infection results in phosphorylation of several nucleoporins including Nup214, Nup98, Nup62, and Nup53 (Porter and Palmenberg 2009; Porter, Brown and Palmenberg 2010). The nuclear accumulation of Nup93 upon nsp1 expression suggests a novel function of this RNA virus-encoded protein to alter the composition of NPC without disrupting the entire nuclear pore and nuclear envelope. Nup93 is an integral part of the nuclear pore complex and has been shown to impair nuclear growth in reconstituted experiments conducted with the *Xenopus* Nup93 depleted NPC complex (Grandi *et al.* 1997), and results an aberrant nuclear shape upon Nup93 knock-down of HeLa cells (Hawryluk-Gara, Shibuya and Wozniak 2005). In corroboration with the effect of Nup93 in maintaining the nuclear morphology, Nup93 associates on the chromatin to mediate chromatin organization and gene expression (Labade, Karmodiya and Sengupta, 2016). Very little is known about the role of Nup93 in the context of a viral infection except its role in nuclear cytoplasmic export of viral mRNA in influenza virus infected human epithelial lung cells (Furusawa, Yamada and Kawaoka 2018). We do not know if Nup93 displacement by nsp1 has effect on nuclear-cytoplasmic localization of proteins other than nucleolin and host mRNA.

To the best of our knowledge, we believe nsp1's ability to disrupt nuclear-cytoplasmic transport has not been reported previously. However, in the context of the whole virus, SARS-CoV protein ORF-6 binds to the nuclear pore complex interacting protein B3 (NPIP3) and enhance nuclear translocation of STAT-1 (Huang *et al.* 2017). Our results showed that nuclear-cytoplasmic distribution of several heterogenous nuclear ribonucleoproteins remains unperturbed, but localization of nucleolin is significantly modified. Nucleolin, a 710 amino acid long protein, contains a C-terminal region with an arginine/glycine-rich domain (RGG), which is used for its interaction with mRNA. A bipartite NLS allows nucleolin to follow the classical import pathway by binding adaptor importin α and the receptor importin β (Schmidt-Zachmann and Nigg 1993). On the other hand, hnRNPs contain a glycine-rich motif known as the M9 NLS, and is driven by transportin for their localization (Nakielny *et al.* 1996). Nucleolin is a RNA binding protein that resides primarily in the nucleus. However, viral perturbation of nucleolin has been demonstrated in the poliovirus. (Waggoner and Sarnow 1998) Nucleolin interacts with mRNA at the 5'-UTR and the 3'-UTR regions to alter their stability and translational efficiency. Ghisolfi-Nieto *et al.* established a range of RNA sequences that interact with nucleolin, and showed UCCCCGA to be the major binding site for the protein (Ghisolfi-Nieto *et al.* 1996). Nucleolin affects stability and translation of mRNA, while binding to the 5'-UTR often dampens translation, an interaction with the 3'-UTR enhances gene expression. Expression of GAST mRNA, corresponding to the gastrointestinal hormone gastrin, is regulated by several proteins including nucleolin, poly(C)-binding protein, and hnRNPK (Lee *et al.* 2007). Expression of prostaglandin endoperoxide H synthase-1 is also regulated by nucleolin binding to the 5'-UTR (Bunimov *et al.* 2007). Nucleolin binds to the 5'-UTR of the tumor suppressor p53 mRNA along with ribosomal protein L26, and regulates translation (Chen, Guo and Kastan 2012; Ghisolfi-Nieto *et al.* 1996; Schmidt-Zachmann and Nigg 1993; Terrier *et al.* 2016; Waggoner and Sarnow 1998). In SARS coronavirus, nsp1 binds to the 40S ribosome at the 5'-UTR of a vast selection of mRNA and promotes translational inhibition and RNA cleavage (Huang *et al.* 2011). Under the same condition,

an RNA hairpin in the 5'-UTR of SARS coronavirus mRNA prevents cleavage and degradation of the viral RNA. Deletion of this RNA hairpin sequence destabilizes SARS coronavirus mRNA, suggesting that virus uses a mechanism to subvert degradation of its own RNA. Similar to nsp1, another host shutoff protein, SOX, of Kaposi's sarcoma-associated virus (KSHV) promotes cleavage and degradation of wide range of host mRNAs. Selected mRNAs that escapes SOX-mediated degradation include interleukin-6 (IL-6). Muller et al. demonstrated that IL-6 RNA binds to nucleolin which is relocalized into the cytoplasm during the lytic phase of KSHV infection, and protects IL-6 from SOX-mediated degradation. Moreover, cells expressing a subgenomic replicon of SARS-CoV showed increased level of nucleolin in stable isotope labeling by amino acid in cell culture (SILAC) followed by mass spectrometry experiment (Zhang *et al.* 2010). Since nsp1 triggers cleavage and degradation of a majority of host mRNAs while its own genomic RNA is protected, increased amount of nucleolin in the cytoplasm may alleviate the function of nsp1 during host shutoff by differential binding to different RNA sequences. Understanding the role of nucleolin binding to various mRNA sequences including the viral RNA in the presence of nsp1 will uncover the role of nucleolin in host shutoff.

MATERIALS AND METHODS

Plasmids and Cell culture

pCAGGS-nsp1-Myc, pCAGGS-KH-Myc, and pGEX-nsp1 plasmids used in this study are kind gifts from Dr. Shinji Makino (University of Texas Medical Branch). EGFP-NLS plasmid is a kind gift from Dr. Kurt Gustin (University of Arizona, College of Medicine – Phoenix). Mutations were generated in pGEX-nsp1 to create two separate mutations, R124A/K125A and K164A/H165A. HEK cells were cultured in Dulbecco Modified Eagle Medium with 10% fetal bovine serum and 1% antibiotics in a 5% CO₂ incubator. 50-60% confluent cells in the 6-well plates were transfected with 0.5 µg nsp1 or mutant plasmids using Fugene6 in 3:1 ratio following manufacturer's protocol. Cells were either collected for fractionation experiment or were used for immunofluorescence using a slightly modified protocol (see below).

Antibodies

Antibodies were obtained from Santa Cruz Biotechnology: Nup93 (E-8), Nup88 (H-7), Lamin A/C (E-1), nucleolin C23 (H-6), GAPDH (6C5), and Myc (9E10) AlexaFluor647. Primary antibody was used at a 1:100 dilution for immunofluorescence and at a 1:1000 dilution for western blot.

Whole Cell Extract Preparation

The extract was prepared from five 10 cm dishes containing fully confluent HEK cells. The cell pellet was resuspended in 5 pellet volumes of extract buffer (10 mM HEPES, 60 mM KCl, 1 mM EDTA, 0.075% (v/v) NP40, 1 mM DTT, and 1 mM PMSF, pH 7.6), and was incubated on ice for 10 minutes followed by sonication at 35% intensity using three 10 second pulses at 4 °C. Extract was collected after centrifugation of the above mixture at 15000 rpm.

GST and anti-Myc pull down of nsp1 complexes

250 mL of *E. coli* BL21 cultures carrying pGEX-nsp1, pGEX-KH, pGEX-RK, and Taq polymerase plasmids were grown separately to OD₆₀₀ of ~0.6 and were induced with 0.2 mM IPTG. Growth was continued at 30 °C overnight and cells were collected by centrifuging at 6000x g for 10 minutes. Cells were lysed with 12.5 mL lysis buffer (1X PBS, 0.05% NP-40, 0.25 mg/mL lysozyme) and were sonicated at 35% output for 20 seconds with 5-second pulses followed by centrifugation at 8000 rpm for 20 minutes. Separately, 200 µL of glutathione resin (G-Biosciences) was washed 4 times with 10 bead volumes of PBS following the manufacturer's protocol. Four sets of glutathione resin were incubated with BSA followed by two more washes. 12.5 mL of the supernatant (from earlier centrifugation) containing the respective proteins were incubated with glutathione resin for 1 hour followed by another 4 washes each with 10 volumes of buffer. 7.5 mL of pre-cleared whole cell extract was added to each GST-tagged protein and was incubated for 4 hours. Resin-bound protein complexes were washed for 6 times with PBS and proteins were eluted with 750 µL of 10 mM glutathione solution following the manufacturer's protocol. The protein mixture was concentrated using a spin column and were separated using a 4-20% pre-cast gel (GenScript). Gel slices were excised for LC-MS/MS study.

Anti-Myc immunoprecipitation was done from HEK cells expressing pCAGGS-nsp1-Myc and pCAGGS-KH-Myc for 24 hours. To match the expression of both wildtype nsp1 and the mutant, one-sixth amount of mutant plasmid was used during the transfection. To capture protein-protein interactions under cellular condition, cells were treated with 0.2% formaldehyde at room temperature for 10 minutes followed by quenching of extra formaldehyde using 0.25M glycine. Extract was prepared using buffer containing 150 mM KCl, 10 mM HEPES, 3 mM MgCl₂, 10% glycerol, 0.5% NP-40 and 2 mM DTT followed by brief sonication to disrupt large complexes. Extract was first precleared with protein A/G agarose beads followed by immunoprecipitation using anti-Myc antibody attached to protein A/G beads by overnight incubation in the presence of protease inhibitor and 0.1 mM DTT. Beads were washed six times using 10 bead volume of phosphate buffer saline. Immunoprecipitate was treated with 1x Laemmli buffer at 80 °C

for 5 minutes before separating proteins using a 4-20% pre-cast gel. Western blot was carried out using specific antibodies at 1:1000 dilutions.

Mass Spectrometry

Identification of proteins that differentially bound to nsp1 and not the inactive mutant were calculated from peptide peak intensities using the MaxQuant algorithm. In short, gel bands were excised and destained. Proteins were reduced in 10 mM dithiothreitol (Thermo Scientific, Rockford, IL) at 55°C, and alkylated in 25 mM iodoacetamide (Thermo) for 30 minutes at room temperature in the dark. The protein was digested with trypsin (Sigma, 100 ng) overnight at 37°C. Digestion was quenched by the addition of trifluoroacetic acid to a final concentration of 1%, and peptides were extracted from the gel and dried. Peptides were resuspended and the entire band was injected onto a trap column and separated with a 75 μ m x 30 cm analytical column at 60°C using a gradient from 5% B to 40% B in 180 min (Solvent A: 0.2% formic acid in 2% acetonitrile; Solvent B: 2% formic acid in 98% acetonitrile) on a U3000 nano LC system. The flow rate was 180 nL/min. Mass spectra were acquired on an Orbitrap Elite (Thermo Scientific) in the data dependent mode with one FTMS survey scan, mass range of m/z 400-1700 Th, followed by collisional dissociation of the ten most intense ions and detection in the ion trap. Data was searched using MaxQuant v.1.6.1.5 against a Human UniProt protein database (71,722 sequences, updated January 2018) including common contaminants. LC-MS/MS analyses were performed for each condition and searched together matching between runs with a 0.7 min window. At least two peptides were required for protein quantification with at least one unique peptide. Intensity measurements were quantified and normalized by the MaxQuant LFQ algorithm. Binary comparisons of log₂ transformed LFQ protein peak intensities yielded proteins that were differentially enriched in each affinity purification. The peptide sequence corresponding to Nup93 is MDTEGFGELLQQAEQLAAETEGISELPHVER. It is the N-term of Nup93 and covers amino acids 1-31. The mass of the peptide is 3426.6249, and it has a N-term acetyl group and oxidized methionine. We detected and sequenced the +3 charge state of this peptide with a m/z of 1163.5.

Nuclear Cytoplasmic Fractionation

Cell pellets from HEK cells were first resuspended in 5 pellet volumes of CE buffer (10 mM HEPES, 60 mM KCl, 1 mM EDTA, 0.075% (v/v) NP40, 1 mM DTT, and 1 mM PMSF, adjusted to pH 7.6) and were left to incubate on ice for 3 min. The cell suspension was centrifuged using a microcentrifuge at 1500 rpm for 4 min. The supernatant was collected as the cytoplasmic extract into a clean tube. The nuclei were washed with 5 cell volumes of CE buffer without detergent. Next, 1 pellet volume NE buffer (20 mM Tris Cl, 420 mM NaCl, 1.5 mM MgCl₂, 0.2 mM EDTA, 1 mM PMSF, and 25% (v/v) glycerol, pH 8.0) was added to the nuclear pellet and was sonicated at 35% input using three 10 second pulses followed by a centrifugation at 15000 rpm. The supernatant was collected as the nuclear extract. Both extracts were boiled with Laemmli buffer before loading to a gel.

Immunofluorescence

Cover slips were coated with 2% polyglycine solution before plating the cells in 12 well plates. HEK cells were transfected with 0.25 μ g pCAGGS-nsp1-Myc or the corresponding K164A/H165A mutant. For the EGFP-NLS experiments 1 μ g of EGFP-NLS plasmid was transfected to each well of a 12 well plate using Fugene6 followed by a second transfection with EGFP-NLS three days later. Two days later, cells were transfected with 0.25 μ g of pCAGGS-nsp1-Myc plasmid per well. 24 hours post-transfection, (unless otherwise specified) cells were washed twice with 500 μ L 1X PBS and immobilized using 500 μ L of 4% formaldehyde/in PBS for 10 minutes at room temperature. Cells were permeabilized with 500 μ L of 0.5% Triton-X in 1X PBS to each well for 5 minutes at 4°C. Cells were washed for 3 times with 1X PBS and blocked with 200 μ L of 1% BSA in PBS for 30 minutes at room temperature. Cells were incubated with

250 μ L of 1:100 dilution of specified primary antibody in 1% BSA/1X PBS solution overnight at 4 °C. The antibody was discarded and cells were washed with 1X PBS three times. Next, they were incubated with 250 μ L of 1:400 dilution of the secondary antibody in 1% BSA/1X PBS solution for 40 minutes followed by three 1X PBS washes. The cover slip was briefly dried before adding mounting media containing DAPI. Images were taken using Leica confocal microscope using 63x magnification.

ACKNOWLEDGEMENTS

We would like to thank Dr. Shinji Makino (University of Texas Medical Branch) and Dr. Kurt Gustin (University of Arizona, College of Medicine – Phoenix) for providing reagents. We would like to thank Dr. Lauren Ball and Jenifer Bethard at Medical University of South Carolina and MUSC Mass Spectrometry Facility and NIH/ S10 D010731 (Orbitrap Elite ETD Mass Spectrometer). Fareeha Abrar and Maya Dodhia were supported by the South Carolina Independent Schools and Colleges Summer Fellows award. We thank Isha Patel for her help, and Prem Chockalingam and Jessica Adams for helpful discussions. We would also like to thank the South Carolina INBRE Bioinformatics Pilot Project award. Research reported in this publication was supported by the National Institute of General Medical Sciences of the National Institute of Health under the award number P20GM103499.

The authors declare that they have no conflict of interest with the content of this article.

REFERENCES

- Ao, Z., Jayappa, K. D., Wang, B., Zheng, Y., Wang, X., Peng, J. and Yao, X. 2012. 'Contribution of host nucleoporin 62 in HIV-1 integrase chromatin association and viral DNA integration', *J Biol Chem*, 287(13), pp. 10544-55.
- Bernad, R., Engelsma, D., Sanderson, H., Pickersgill, H. and Fornerod, M. 2006. 'Nup214-Nup88 nucleoporin subcomplex is required for CRM1-mediated 60 S preribosomal nuclear export', *J Biol Chem*, 281(28), pp. 19378-86.
- Bernad, R., van der Velde, H., Fornerod, M. and Pickersgill, H. 2004. 'Nup358/RanBP2 attaches to the nuclear pore complex via association with Nup88 and Nup214/CAN and plays a supporting role in CRM1-mediated nuclear protein export', *Mol Cell Biol*, 24(6), pp. 2373-84.
- Borah, S., Darricarrère, N., Darnell, A., Myoung, J. and Steitz, J. A. 2011. 'A viral nuclear noncoding RNA binds re-localized poly(A) binding protein and is required for late KSHV gene expression', *PLoS Pathog*, 7(10), pp. e1002300.
- Bunimov, N., Smith, J. E., Gosselin, D. and Laneuville, O. 2007. 'Translational regulation of PGHS-1 mRNA: 5' untranslated region and first two exons conferring negative regulation', *Biochim Biophys Acta*, 1769(2), pp. 92-105.
- Chen, J., Guo, K. and Kastan, M. B. 2012. 'Interactions of nucleolin and ribosomal protein L26 (RPL26) in translational control of human p53 mRNA', *J Biol Chem*, 287(20), pp. 16467-76.
- Copeland, A. M., Newcomb, W. W. and Brown, J. C. 2009. 'Herpes simplex virus replication: roles of viral proteins and nucleoporins in capsid-nucleus attachment', *J Virol*, 83(4), pp. 1660-8.
- Di Nunzio, F., Danckaert, A., Fricke, T., Perez, P., Fernandez, J., Perret, E., Roux, P., Shorte, S., Charneau, P., Diaz-Griffero, F. and Arhel, N. J. 2012. 'Human nucleoporins promote HIV-1 docking at the nuclear pore, nuclear import and integration', *PLoS One*, 7(9), pp. e46037.

- Furusawa, Y., Yamada, S. and Kawaoka, Y. 2018. 'Host Factor Nucleoporin 93 Is Involved in the Nuclear Export of Influenza Virus RNA', *Front Microbiol*, 9, pp. 1675.
- Ghisolfi-Nieto, L., Joseph, G., Puvion-Dutilleul, F., Amalric, F. and Bouvet, P. 1996. 'Nucleolin is a sequence-specific RNA-binding protein: characterization of targets on pre-ribosomal RNA', *J Mol Biol*, 260(1), pp. 34-53.
- Grandi, P., Dang, T., Pané, N., Shevchenko, A., Mann, M., Forbes, D. and Hurt, E. 1997. 'Nup93, a vertebrate homologue of yeast Nic96p, forms a complex with a novel 205-kDa protein and is required for correct nuclear pore assembly', *Mol Biol Cell*, 8(10), pp. 2017-38.
- Gustin, K. E. and Sarnow, P. 2001. 'Effects of poliovirus infection on nucleo-cytoplasmic trafficking and nuclear pore complex composition', *EMBO J*, 20(1-2), pp. 240-9.
- Gustin, K. E. and Sarnow, P. 2002. 'Inhibition of nuclear import and alteration of nuclear pore complex composition by rhinovirus', *J Virol*, 76(17), pp. 8787-96.
- Hawryluk-Gara, L. A., Shibuya, E. K. and Wozniak, R. W. 2005. 'Vertebrate Nup53 interacts with the nuclear lamina and is required for the assembly of a Nup93-containing complex', *Mol Biol Cell*, 16(5), pp. 2382-94.
- Huang, C., Lokugamage, K. G., Rozovics, J. M., Narayanan, K., Semler, B. L. and Makino, S. 2011. 'SARS coronavirus nsp1 protein induces template-dependent endonucleolytic cleavage of mRNAs: viral mRNAs are resistant to nsp1-induced RNA cleavage', *PLoS Pathog*, 7(12), pp. e1002433.
- Huang, S. H., Lee, T. Y., Lin, Y. J., Wan, L., Lai, C. H. and Lin, C. W. 2017. 'Phage display technique identifies the interaction of severe acute respiratory syndrome coronavirus open reading frame 6 protein with nuclear pore complex interacting protein NPIP3 in modulating Type I interferon antagonism', *J Microbiol Immunol Infect*, 50(3), pp. 277-285.
- Ibarra, A., Benner, C., Tyagi, S., Cool, J. and Hetzer, M. W. 2016. 'Nucleoporin-mediated regulation of cell identity genes', *Genes Dev*, 30(20), pp. 2253-2258.
- Jauregui, A. R., Savalia, D., Lowry, V. K., Farrell, C. M. and Wathelet, M. G. 2013. 'Identification of residues of SARS-CoV nsp1 that differentially affect inhibition of gene expression and antiviral signaling', *PLoS One*, 8(4), pp. e62416.
- Kamitani, W., Huang, C., Narayanan, K., Lokugamage, K. G. and Makino, S. 2009. 'A two-pronged strategy to suppress host protein synthesis by SARS coronavirus Nsp1 protein', *Nat Struct Mol Biol*, 16(11), pp. 1134-40.
- Kamitani, W., Narayanan, K., Huang, C., Lokugamage, K., Ikegami, T., Ito, N., Kubo, H. and Makino, S. 2006. 'Severe acute respiratory syndrome coronavirus nsp1 protein suppresses host gene expression by promoting host mRNA degradation', *Proc Natl Acad Sci U S A*, 103(34), pp. 12885-90.
- Knockenbauer, K. E. and Schwartz, T. U. 2016. 'The Nuclear Pore Complex as a Flexible and Dynamic Gate', *Cell*, 164(6), pp. 1162-1171.
- Labade, A. S., Karmodiya, K. and Sengupta, K. 2016. 'HOXA repression is mediated by nucleoporin Nup93 assisted by its interactors Nup188 and Nup205', *Epigenetics Chromatin*, 9, pp. 54.
- Le Sage, V. and Moulard, A. J. 2013. 'Viral subversion of the nuclear pore complex', *Viruses*, 5(8), pp. 2019-42.
- Lee, P. T., Liao, P. C., Chang, W. C. and Tseng, J. T. 2007. 'Epidermal growth factor increases the interaction between nucleolin and heterogeneous nuclear ribonucleoprotein K/poly(C) binding protein 1 complex to regulate the gastrin mRNA turnover', *Mol Biol Cell*, 18(12), pp. 5004-13.
- Lokugamage, K. G., Narayanan, K., Huang, C. and Makino, S. 2012. 'Severe acute respiratory syndrome coronavirus protein nsp1 is a novel eukaryotic translation inhibitor that represses multiple steps of translation initiation', *J Virol*, 86(24), pp. 13598-608.
- Lokugamage, K. G., Narayanan, K., Nakagawa, K., Terasaki, K., Ramirez, S. I., Tseng, C. T. and Makino, S. 2015. 'Middle East Respiratory Syndrome Coronavirus nsp1 Inhibits Host Gene Expression by Selectively

- Targeting mRNAs Transcribed in the Nucleus while Sparing mRNAs of Cytoplasmic Origin', *J Virol*, 89(21), pp. 10970-81.
- McBride, A. E., Schlegel, A. and Kirkegaard, K. 1996. 'Human protein Sam68 relocalization and interaction with poliovirus RNA polymerase in infected cells', *Proc Natl Acad Sci U S A*, 93(6), pp. 2296-301.
- Mühlbauer, D., Dzieciolowski, J., Hardt, M., Hocke, A., Schierhorn, K. L., Mostafa, A., Müller, C., Wisskirchen, C., Herold, S., Wolff, T., Ziebuhr, J. and Pleschka, S. 2015. 'Influenza virus-induced caspase-dependent enlargement of nuclear pores promotes nuclear export of viral ribonucleoprotein complexes', *J Virol*, 89(11), pp. 6009-21.
- Naetar, N., Ferraioli, S. and Foisner, R. 2017. 'Lamins in the nuclear interior - life outside the lamina', *J Cell Sci*, 130(13), pp. 2087-2096.
- Nakielny, S., Siomi, M. C., Siomi, H., Michael, W. M., Pollard, V. and Dreyfuss, G. 1996. 'Transportin: nuclear transport receptor of a novel nuclear protein import pathway', *Exp Cell Res*, 229(2), pp. 261-6.
- Narayanan, K., Huang, C., Lokugamage, K., Kamitani, W., Ikegami, T., Tseng, C. T. and Makino, S. 2008. 'Severe acute respiratory syndrome coronavirus nsp1 suppresses host gene expression, including that of type I interferon, in infected cells', *J Virol*, 82(9), pp. 4471-9.
- Park, N., Katikaneni, P., Skern, T. and Gustin, K. E. 2008. 'Differential targeting of nuclear pore complex proteins in poliovirus-infected cells', *J Virol*, 82(4), pp. 1647-55.
- Park, N., Skern, T. and Gustin, K. E. 2010. 'Specific cleavage of the nuclear pore complex protein Nup62 by a viral protease', *J Biol Chem*, 285(37), pp. 28796-805.
- Porter, F. W., Brown, B. and Palmenberg, A. C. 2010. 'Nucleoporin phosphorylation triggered by the encephalomyocarditis virus leader protein is mediated by mitogen-activated protein kinases', *J Virol*, 84(24), pp. 12538-48.
- Porter, F. W. and Palmenberg, A. C. 2009. 'Leader-induced phosphorylation of nucleoporins correlates with nuclear trafficking inhibition by cardioviruses', *J Virol*, 83(4), pp. 1941-51.
- Schmidt-Zachmann, M. S. and Nigg, E. A. 1993. 'Protein localization to the nucleolus: a search for targeting domains in nucleolin', *J Cell Sci*, 105 (Pt 3), pp. 799-806.
- Sevajol, M., Subissi, L., Decroly, E., Canard, B. and Imbert, I. 2014. 'Insights into RNA synthesis, capping, and proofreading mechanisms of SARS-coronavirus', *Virus Res*, 194, pp. 90-9.
- Tanaka, T., Kamitani, W., DeDiego, M. L., Enjuanes, L. and Matsuura, Y. 2012. 'Severe acute respiratory syndrome coronavirus nsp1 facilitates efficient propagation in cells through a specific translational shutoff of host mRNA', *J Virol*, 86(20), pp. 11128-37.
- Terrier, O., Carron, C., De Chasse, B., Dubois, J., Traversier, A., Julien, T., Cartet, G., Proust, A., Hacot, S., Ressnikoff, D., Lotteau, V., Lina, B., Diaz, J. J., Moules, V. and Rosa-Calatrava, M. 2016. 'Nucleolin interacts with influenza A nucleoprotein and contributes to viral ribonucleoprotein complexes nuclear trafficking and efficient influenza viral replication', *Sci Rep*, 6, pp. 29006.
- Vollmer, B. and Antonin, W. 2014. 'The diverse roles of the Nup93/Nic96 complex proteins - structural scaffolds of the nuclear pore complex with additional cellular functions', *Biol Chem*, 395(5), pp. 515-28.
- Waggoner, S. and Sarnow, P. 1998. 'Viral ribonucleoprotein complex formation and nucleolar-cytoplasmic relocalization of nucleolin in poliovirus-infected cells', *J Virol*, 72(8), pp. 6699-709.
- Zhang, L., Zhang, Z. P., Zhang, X. E., Lin, F. S. and Ge, F. 2010. 'Quantitative proteomics analysis reveals BAG3 as a potential target to suppress severe acute respiratory syndrome coronavirus replication', *J Virol*, 84(12), pp. 6050-9.

FIGURE LEGENDS

Figure 1: Expression and immunoprecipitation of nsp1. A) Nsp1 expression and localization in HEK cells was conducted 24 hours post-transfection. Cells were transfected with pCAGGS-nsp1-Myc or the corresponding K164A/H165A plasmid. The Myc-tag was identified using anti-MycAlexaFluor647 primary antibody. B) Expression of Myc-tagged nsp1 and K164A/H165A in HEK cells were detected using the anti-Myc antibody. C) Myc-tagged nsp1 or mock transfected HEK cells were used for cell extract preparation after 24 hours of transfection. Anti-Myc antibody was used on protein A/G agarose beads for immunoprecipitation followed by western blot using anti-Myc and anti-Nup93 antibody. D) anti-Myc immunoprecipitation was carried out as described above using Myc-tagged nsp1 and K164A/H165A mutant followed by western blot.

Figure 2: Nup93 localization changes in the presence of nsp1. A) Cells were transfected with pCAGGS-nsp1 or the corresponding mutant plasmid. Nup93 localization was monitored 24 hours post-transfection with anti-Nup93 primary and anti-mouse AlexaFluor 488 secondary antibodies. Images were collected with Leica confocal microscope using 63x objective and images of all three samples were collected using constant laser intensity for DAPI, AlexaFluor488 and AlexaFluor647. B) Images of 17 Z-stacks were collected for each sample. Z 10-12 were selected for nucleoplasmic fluorescent density calculation. ImageJ was used to calculate nuclear density of Nup93 from two independent biological replicates (n=2) totaling 50 cells for each sample. The scale bar is set at 20 μm . C) Mean density and statistical distribution was collected using GraphPad Prism7 program using one-way ANOVA for multiple samples. D) Nuclear cytoplasmic fractionation of cell expressing pCAGGS-nsp1 or the corresponding mutant were performed followed by SDS gel and western blot using anti-Nup93 and anti-hnRNPK antibodies.

Figure 3: Nuclear envelope and the nucleoporin Nup88 are unaltered upon nsp1 expression. A) Nuclear Lamin A/C was identified using anti-Lamin A/C antibody 24 hours after nsp1 plasmid transfection. B) Nuclear pore protein Nup88 was identified using anti-Nup88 antibody 24 hours after nsp1 transfection. Images were collected with Leica confocal microscope using 63x objective.

Figure 4: Nup93 localization at multiple time intervals suggests that Nup93 localization is dependent on the presence of nsp1. A) Nup93 is not degraded in the presence of nsp1. Nsp1 and K164A/H165A expressing cells were treated with 100 μM cyclohexamide followed by analysis of Nup93 with western blot using anti-Nup93 antibody. Nup93 does not undergo rapid degradation in the presence of nsp1. B) Nsp1 expression decreases significantly 40 hours post-transfection. Both nsp1 and K164AH165A levels are compared using western blot with anti-Myc tag and anti-GAPDH. C) Nup93 localization is monitored for 0, 12, 24, and 48 hours post-transfection with pCAGGS-nsp1 or the corresponding mutant plasmid. The scale bar is set at 20 μm . (D) Images of 17 Z-stacks were collected for each sample. Z 10-12 were selected for nucleoplasmic fluorescent density calculation. ImageJ was used to calculate nuclear density of Nup93 from two independent biological replicates. Mean density and statistical distribution was collected using GraphPad Prism7 program using one way Avona for multiple samples.

Figure 5: Nsp1 expression alters nuclear-cytoplasmic localization of nucleolin. A) Western blot analyses of nuclear and cytoplasmic distribution of nucleolin, hnRNPK, hnRNP and hnRNPE1/E2 in the presence and absence of nsp1 and K164A/H165A mutant using specified antibodies. N stands for the nuclear fraction and C stands for the cytoplasmic fraction. B) Quantitative analysis of nuclear vs cytoplasmic ratio of nucleolin and hnRNPK using ImageJ in the presence and absence of nsp1 and K164A/H165A mutant from four independent experiments (n=4).

Figure 1

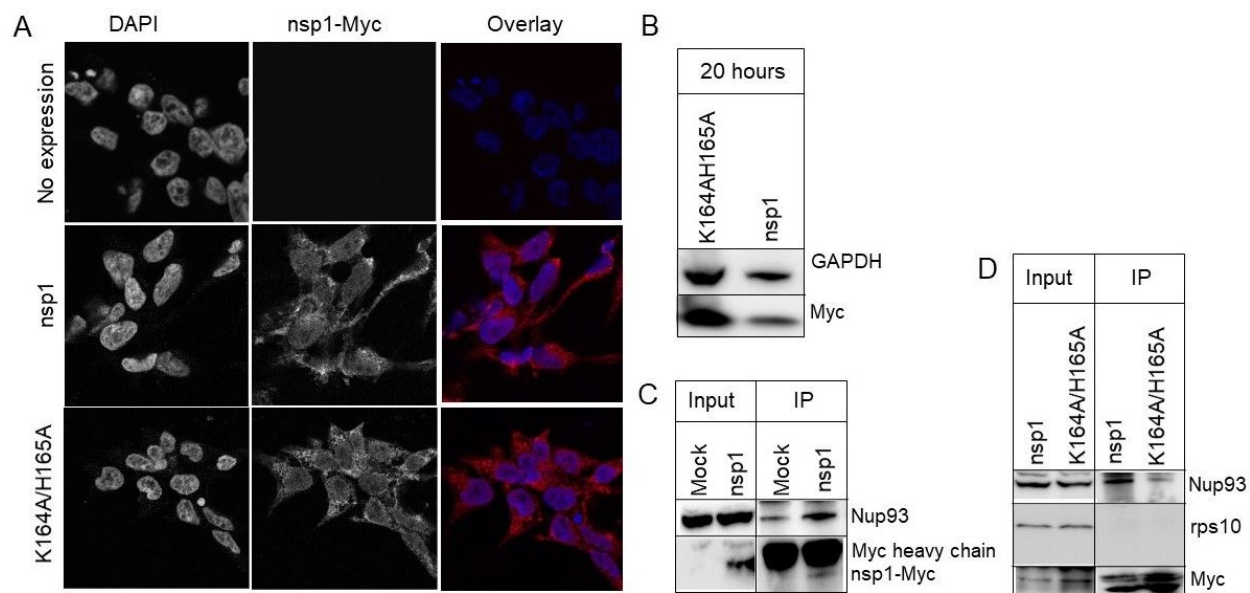


Figure 2

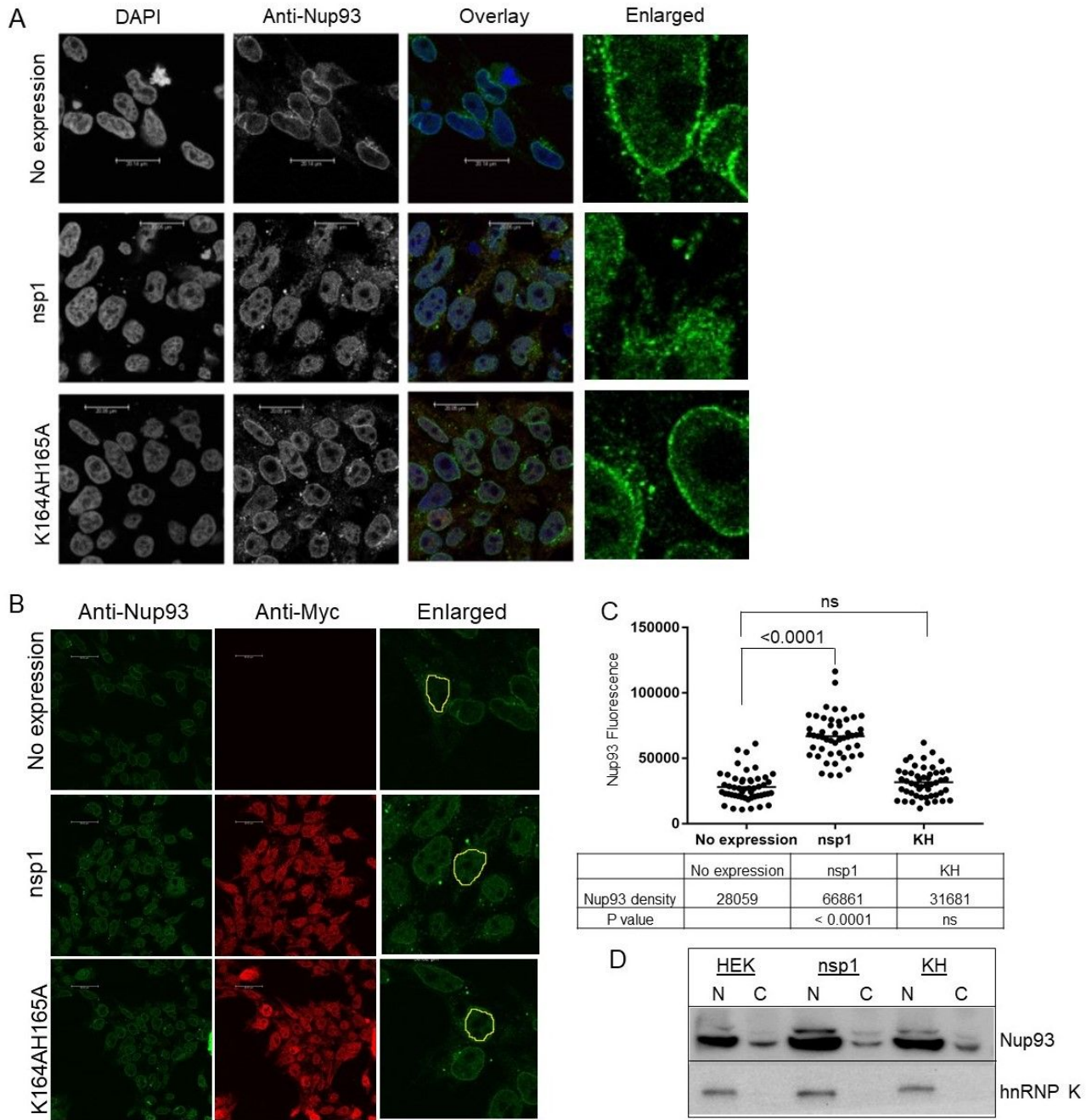


Figure 3

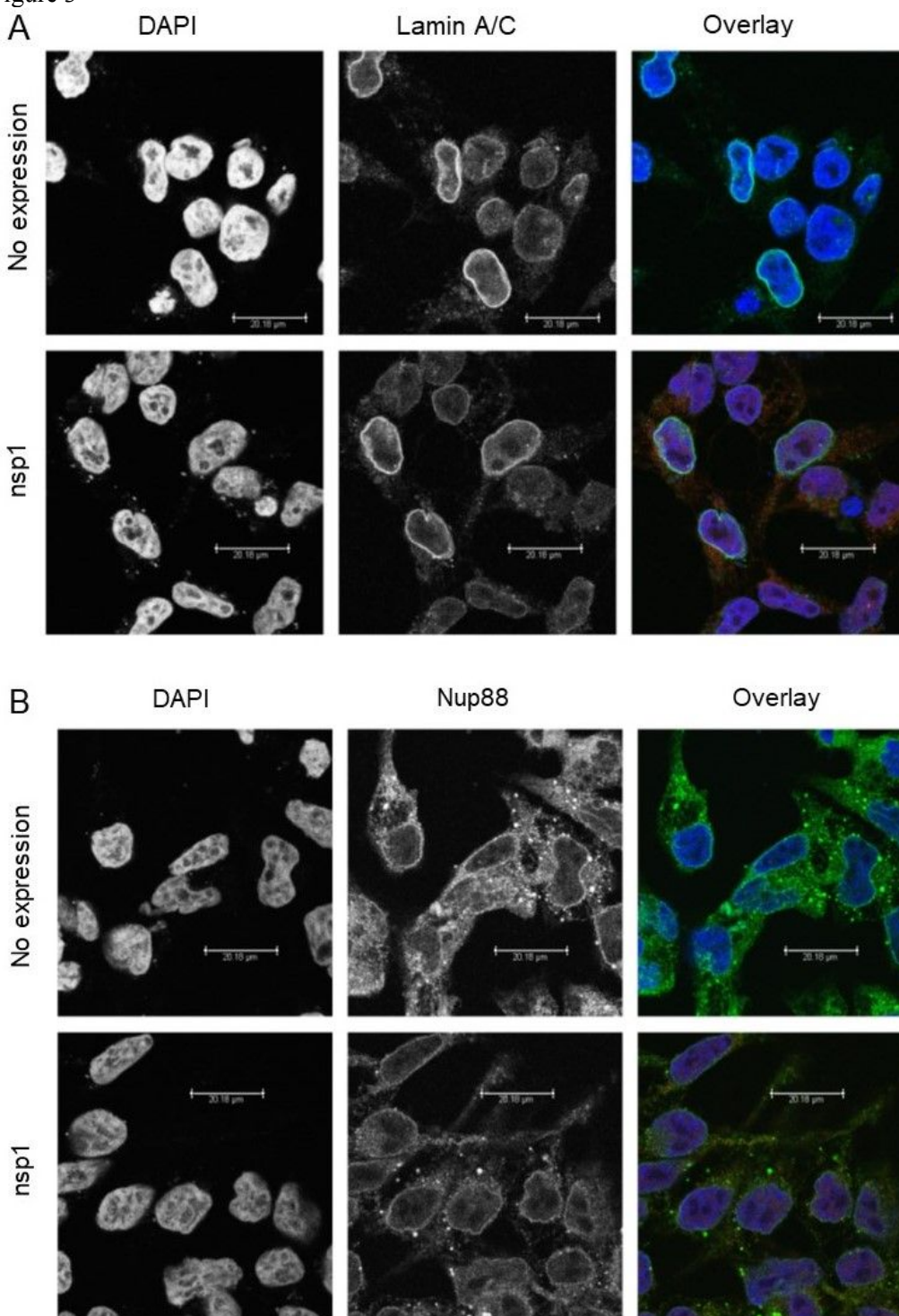


Figure 4

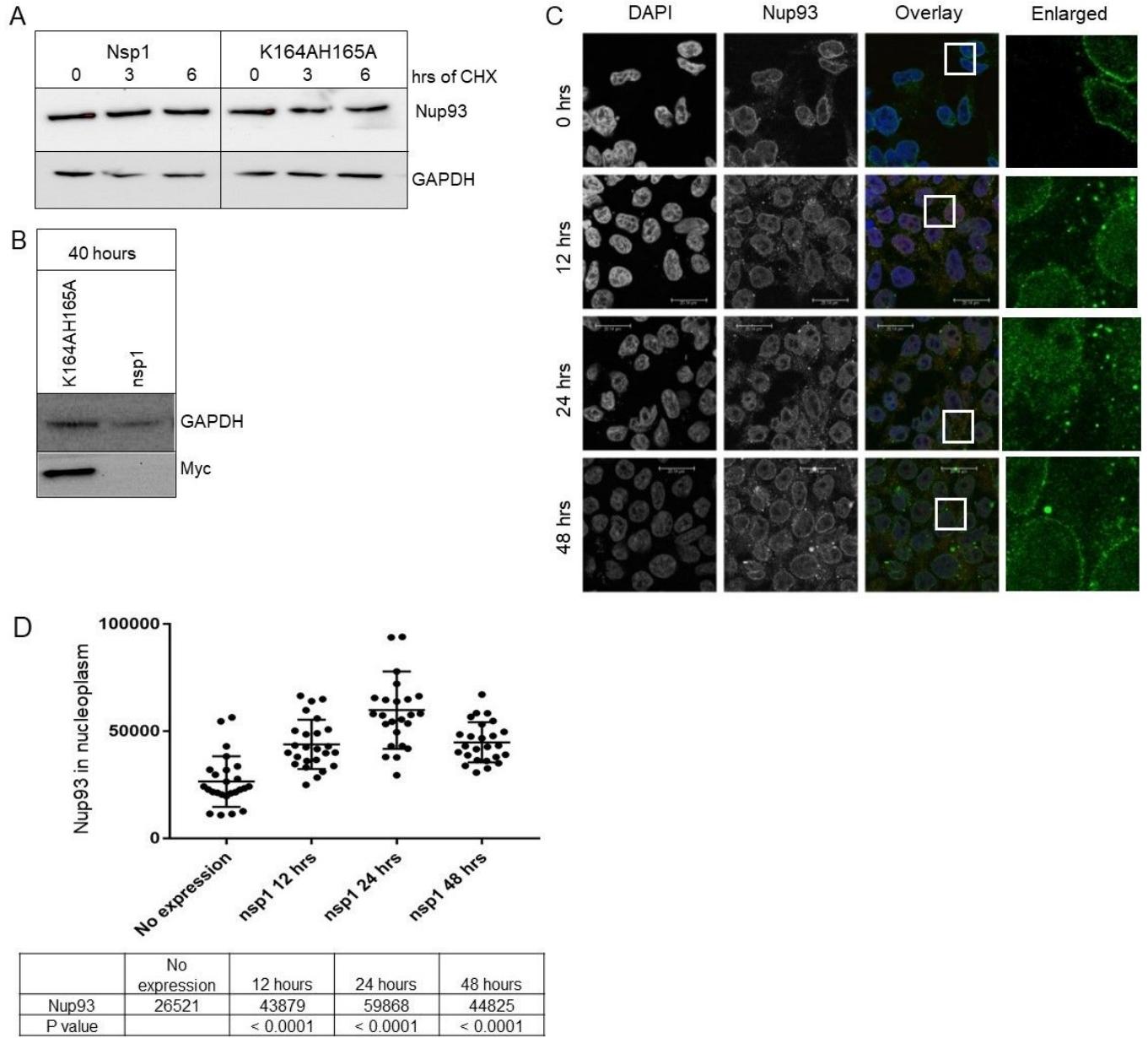


Figure 5

